A Design for Increasing the Capacity Fourfold in NB-IoT Systems using A Modified Symbol Time Compression Approach

Abdulwahid Mohammed[1*], Hassan Mostafa[2] and Abd El-Hady. A. Ammar[3]

[1*]PhD Researcher, Electronics and Communication Engineering Department, Al-Azhar University, Cairo, Egypt. abdulwahid.21@azhar.edu.eg, Orcid: https://orcid.org/0000-0003-1866-430X

[2]Associate Professor, Electronics and Communication Engineering Department, Cairo University, Giza, Egypt. hmostafa@zewailcity.edu.eg, Orcid: https://orcid.org/0000-0003-0043-5007

[3]Professor, Electronics and Communication Engineering Department, Al-Azhar University, Cairo, Egypt. hady42amar@gmail.com, Orcid: https://orcid.org/0000-0003-4176-0666

Received: August 07, 2023; Accepted: October 12, 2023; Published: November 30, 2023

Abstract

One of the most significant obstacles facing the Internet of Things (IoT) is how to offer support for communication to an expanding number of linked items. Narrow-band Internet of Things (NB-IoT), which is currently an aspect of fifth-generation (5G), is a new narrow-band wireless communication technology that has evolved in recent years to address this issue. To save power, NB-IoT currently exploits modulation schemes that are characterized by low order to deliver low data rate. However, as the number of applications dependent on data rate increases, NB-IoT needs to use data rate improvement technologies that do not consume additional power. This paper proposes a design for quadrupling the total number of linked items in the NB-IoT system using a symbol time compression methodology. A modified symbol time compression (MSTC) approach is specifically suggested, which could preserve 75% of the bandwidth (BW) by reducing the symbol time to a quarter (25%). This study suggests a design that uses the MSTC method four times in orthogonal frequency division multiplexing (4-MSTC-OFDM) to take advantage of the unused bandwidth and has the capability to deliver a quadruple quantity of information in comparison to the standard OFDM system. Simulations show that the suggested design (4-MSTC-OFDM) lowers the signal-to-noise ratio (SNR) by 3.9 dB (at BER = 10-6) and 4.4 dB (at BER = 10-4) compared to the OFDM system with 16-QAM (16-QAM-OFDM) when sending the same amount of data over the Rayleigh fading channel and additive white Gaussian noise channel (AWGN). Moreover, the results of simulations indicate that the proposed design possesses an identical BER as the conventional OFDM technique, implying that using the suggested method does not degrade the BER.

Keywords: NB-IoT, CSTC-OFDM, MSTC-OFDM, 4-MSTC-OFDM.

1 Introduction

With the fast evolution of next-generation 5G technologies, extensive studies on massive machine-type communications (mMTCs), enhanced mobile broadband (eMBB), and ultra-reliable low-latency

Journal of Interner Services and Information Security (JISIS), volume: 13, number: 4 (November), pp. 170-184
DOI: *10.58346/JISIS.2023.I4.012*

*Corresponding author: PhD Researcher, Electronics and Communication Engineering Department, Al-Azhar University, Cairo, Egypt.

communications (URLLCs) have attracted significantly increased attention from both academic and business communities (Liu, S., et al., 2019). 5G was first formalized by 3GPP in Release 15 in 2018 (Li, Y., et al., 2017), and implementation by both public and commercial telecom operators started shortly thereafter. For instance, near the end of 2018, Verizon and AT&T launched their first 5G services in the USA (Chen, Y., et al., 2022). The requirements of the three different applications are diverse, as seen in Figure 1. In order to support eMBB, 5G connectivity must deliver high-speed data throughput of up to 10 Gbps. Regarding URLLC, 5G has to support connections that need less than 1 ms of latency for mission-critical operations. For mMTC, 5G is anticipated to provide extremely dense connections (1 million per km2) (Migabo, E. M., et al., 2020). In addition to significant improvements in the aforementioned NR, the appropriate coexistence of various networks, as well as the interoperability of 4G and 5G systems, must be carefully considered (Niu, Y., et al., 2015). On the other hand, low-power wide area (LPWA) technologies, such as narrow-band Internet of Things (NB-IoT) (Martinez, B., et al., 2019), long-range wide area network (LoRaWAN) (Ertürk, M. A., et al., 2019), and SigFox (Zuniga, J. C., et al., 2016), are an important class of 5G networks for massive IoT applications (Mekki, K., et al., 2019). In particular, LPWA technologies are developed with the following objectives: transmission distances of up to 40km, supporting thousands of endpoints per base station (BS), ensuring a battery life of over ten years without the need for recharging, and maintaining module prices of around $5 (Luján, E., et al., 2019).

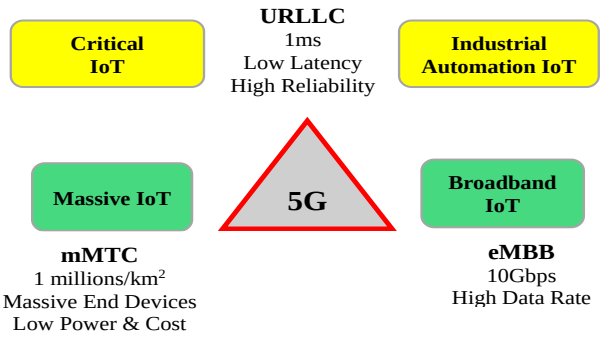

Figure 1: Three Pillars of 5G and Applications Scenarios (Chen, Y., et al., 2022)

NB-IoT is a typical example of a cellular technology based on long-term evolution (LTE) with a system bandwidth of 180 kHz that supports enormous device connections while having low-power and cost-effective features suitable for delay-tolerant IoT applications. Because of its low bandwidth requirements, NB-IoT could be operated in three modes: stand-alone, in-band, and guard-band. In stand-alone mode, NB-IoT may function as a stand-alone carrier over a channel of a global system for mobile communications (GSM) (200 kHz). Nevertheless, NB-IoT works on one physical resource block (PRB) during the transmission of LTE for in-band and guard-band modes (Marini, R., et al., 2022). Since it utilizes the current infrastructure and can be implemented as a firmware upgrade instead of deploying new hardware, the in-band deployment approach would be more effective and economical. In addition to the fundamental LTE design, NB-IoT has been updated with several additional capabilities to better fulfill IoT requirements and work in harmony with the LTE network (Malik, H., et al., 2019). The use of NB-IoT covers several industrial areas, with varying degrees of implementation. This is generally determined by the criticality and amount of trust in NB-IoT. Nevertheless, its utilization is anticipated to grow in the upcoming years, especially with the increased production of NB-IoT modules by numerous suppliers (Dangana, M., et al., 2021). As shown in Figure 2, NB-IoT is used for a variety of purposes in industry. For instance, NB-IoT adoption in the oil and gas sectors comprises product

refinement, distribution, and monitoring. Applications can also be found in smart buildings (Qolomany, B., et al., 2019), smart cities (Javidroozi, V., et al., 2019), smart environmental monitoring systems (Du, R., et al.,2018), smart metering (Wan, L., et al., 2019), and intelligent user services (Nair, V., et al., 2019).

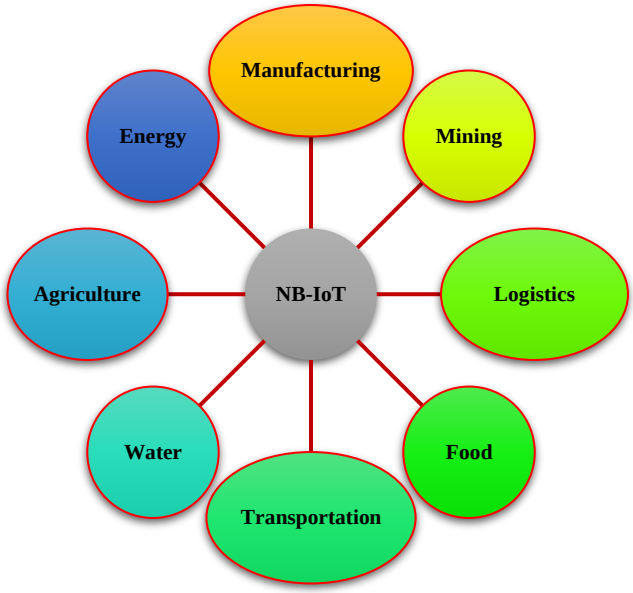

Figure 2: Uses of NB-IoT in Many Industrial Sectors (Dangana, M., et al., 2021)

State of the Art

Despite the benefits of NB-IoT, there are some challenges that require further research. One of the major problems is how to effectively connect a large number of users to NB-IoT systems using the limited available spectrum. Given that NB-IoT is anticipated to function within the same frequency spectrum as LTE, this poses a number of design challenges for radio resources allocating to IoT devices, particularly in the upcoming 5G heterogeneous networks made up of numerous small cells functioning under the macrocells (Caviglione, L., 2021).

As described in (Xu, T., & Darwazeh, I, 2018, September), the authors came up with a way to use NB-IoT that uses a complex signal waveform called non-orthogonal spectrum efficient frequency division multiplexing (SEFDM). In contrast to OFDM, the resultant signal has the potential to improve the transmission rate without necessitating supplementary bandwidth. Based on the obtained simulation results, it is evident that the suggested signal has the potential to enhance the data rate by 25%, specifically in comparison to the OFDM signal. Nevertheless, the lack of orthogonality among the sub-carriers can result in inter-carrier interference (ICI), which in turn requires the receiver to use more power. The suitability of base stations for processing signals in the up-link channels has been noted (Xu, T., & Darwazeh, I, 2018, September). Nevertheless, this approach is impractical as it requires additional processing to be performed on the downlink channels.

Fast-Orthogonal Frequency Division Multiplexing (Fast-OFDM) is employed in (Xu, T., & Darwazeh, I, 2018, June) to reduce the utilized bandwidth in half and increase the number of devices that can be connected by a factor of two. The Fast-OFDM technology reduces the inter-subcarrier spacing by 50% in comparison to a conventional OFDM system, consequently mitigating the degradation in bit error rate (BER). Fast-OFDM, on the other hand, may introduce carrier frequency

offset (CFO). Additionally, it is important to note that the peak-to-average power ratio (PAPR) issue still affects this strategy.

In our previous study (Mohammed, A., El-Bakry, M., et al., 2023), we introduced a method based on symbol time compression (STC) that demonstrated the ability to transport double the amount of data compared to a conventional OFDM system while simultaneously decreasing the needed bandwidth by 50%. Moreover, it enhances system performance through the reduction of the PAPR issue in comparison to Fast-OFDM and conventional OFDM systems. Furthermore, the bit error rate (BER) of our proposed approach exhibits similarity to the BER seen in both Fast-OFDM and conventional OFDM systems. Although the proposed system has the advantage of doubling the data transfer capacity compared to a standard OFDM system, it maintains the same level of complexity. Furthermore, the STC-based methodology introduced in our previous work (Mohammed, A., El-Bakry, M., et al., 2023) exhibits good performance compared to the Fast-OFDM technique discussed in (Xu, T., & Darwazeh, I, 2018, June). This is attributed to the STC-based method's ability to preserve the spacing between subcarriers, hence mitigating the occurrence of carrier frequency offset (CFO).

In (Mohammed, A., et al., 2023), we suggested an effective technique to reduce the bandwidth by 75%; this technique is called Modified-STC (MSTC). By decreasing the required number of sub-carriers, the MSTC technology increases the data rate and reduces power consumption. In contrast to the Fast-OFDM in (Xu, T., & Darwazeh, I, 2018, June), the MSTC approach does not result in a discrepancy in the sampling rate since the distance between each of the sub-carriers remains unaltered. Additionally, the MSTC performs better on the PAPR issue than the Fast-OFDM in (Xu, T., & Darwazeh, I, 2018, June) and the Conventional STC (CSTC) method in (Mohammed, A., El-Bakry, M., et al., 2023).

The researchers in (Liu, X., & Darwazeh, I., 2019, April) suggested a novel signaling technique for NB-IoT wireless networks, referred to as HT-Fast-OFDM. This method combines the Fast-OFDM system with a time orthogonal Hilbert transform (HT) pair. By employing these two orthogonal approaches, the data rate is increased fourfold. The HT-Fast-OFDM scheme provides a fourfold increase in data rate in comparison to an OFDM system applying identical modulation (BPSK) and utilizing the exact same bandwidth, according to their simulation results. However, the HT-Fast-OFDM system may experience a carrier frequency offset (CFO) as a result of the smaller sub-carrier spacing. The complexity of the HT-Fast-OFDM system is also increased by the combining of two orthogonal approaches.

Unlike the earlier studies, the Fast-OFDM in (Xu, T., & Darwazeh, I, 2018, June), and the CSTC-OFDM in (Mohammed, A., El-Bakry, M., et al., 2023), our suggested approach (MSTC-OFDM) in (Mohammed, A., et al., 2023) is suitable for large connections because it reduces the utilized bandwidth to 25% (saving 75% of BW) compared to typical OFDM systems, allowing the unused bandwidth to be used to transmit additional data. Although the MSTC-OFDM approach can save bandwidth by 75% in comparison to a standard OFDM system, the BER remains the same. Moreover, the MSTC-OFDM system is more resistant to CFO and inter-carrier interference because it maintains the same sub-carrier spacing as the Fast-OFDM scheme explained in (Xu, T., & Darwazeh, I, 2018, June).

Contributions

Using the MSTC method from our research (Mohammed, A., et al., 2023), we propose in this article a design called 4-MSTC-OFDM that could transmit quadruple the amount of information as a standard OFDM system by utilizing the bandwidth that isn't being used. To fully use the available bandwidth, the

suggested scheme 4-MSTC-OFDM employs the MSTC technique four times in parallel and simultaneously. The subsequent points provide a summary of the advantages offered by this design:

1. The 4-MSTC-OFDM design offers a fourfold increase in data transmission capacity in comparison to the conventional OFDM system, as well as a twofold increase in capacity when compared to the Fast-OFDM system.
2. The 4-MSTC-OFDM architecture has a similar bit error rate (BER) as Fast-OFDM method and traditional OFDM system.
3. The 4-MSTC-OFDM technique demonstrates superior performance over the Fast-OFDM (Xu, T., & Darwazeh, I, 2018, June) and HT-Fast-OFDM system (Liu, X., & Darwazeh, I., 2019, April) in terms of carrier frequency offset (CFO). This advantage arises from the fact that the 4-MSTC-OFDM approach has no impact on the distance that separates the sub-carriers. Furthermore, the 4-MSTC-OFDM has better performance in terms of complexity compared to the HT-Fast-OFDM, as will be seen in Subsection 3.3.
4. The MSTC-OFDM scheme effectively mitigates the PAPR issue in comparison to the conventional OFDM system by using just 25% of the available bandwidth to transmit an equivalent amount of data. In the event that the whole bandwidth is used, the proposed design (4-MSTC-OFDM) transfers four times the amount of information as the standard OFDM system. However, it is expected that the PAPR values for both the conventional OFDM and the proposed design would be about equal. Consequently, the use of companding techniques (Mohammed, A., et al., 2021) may be employed in conjunction with the suggested design (4-MSTC-OFDM) to optimize system performance and mitigate the problem of PAPR. This study utilizes the Mu-law companding approach (Mohammed, A., et al., 2018, August) in conjunction with the proposed design (4-MSTC-OFDM) in order to mitigate the issue of PAPR in the system.

The subsequent sections of this article are structured in the following manner: Section 2 provides a description of the system model for the proposed design (4-MSTC-OFDM). This includes a detailed review of both the MSTC and MSTE system models. Section 3 presents the results of the simulation along with accompanying remarks. Section 4 offers a comprehensive summary of the research, highlighting the advantages associated with the proposed design.

2 System Model of the Proposed Design (4-MSTC-OFDM)

The model of the transceiver system for the suggested design (4-MSTC-OFDM) is seen in Figure 3. To fully exploit the bandwidth, the suggested design (4-MSTC-OFDM) employs four parallel instances of MSTC technology on the transmitter side and four parallel instances of MSTE technology on the receiver side to recover the data that was transmitted. The 4-MSTC-OFDM design, as shown in Figure 3, is made up of four similar units, each of which includes a data source, serial to parallel block (S/P), MSTC methodology, and inverse fast Fourier transform (IFFT) block.

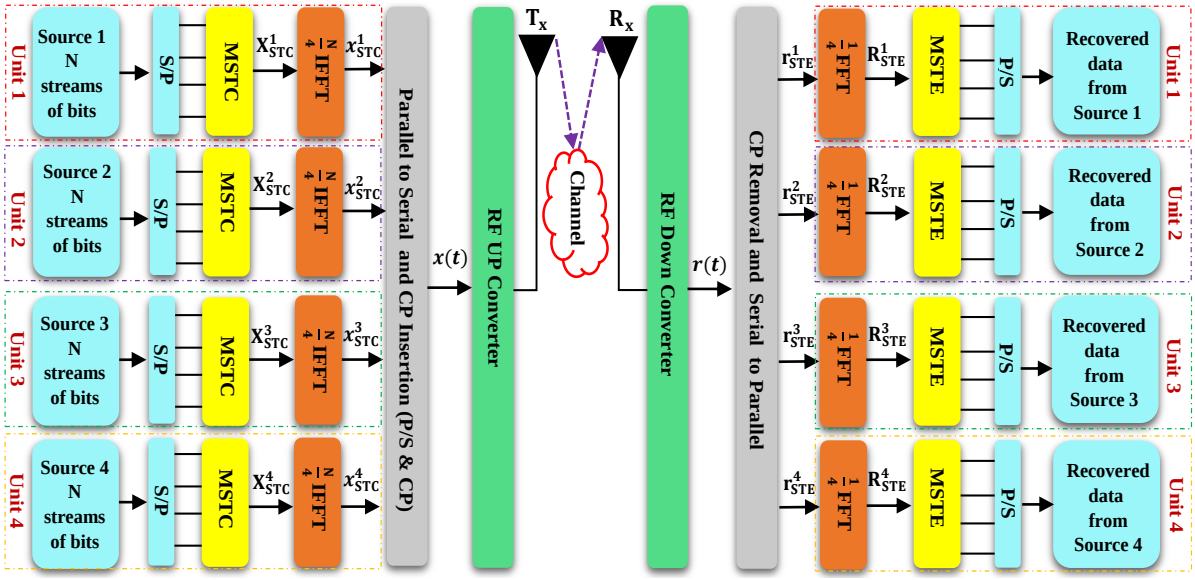

Figure 3: Schematic Representation of the Proposed Design (4-MSTC-OFDM)

The input data is first passed through the S/P block in each unit. Then, it is processed by using the MSTC block in each unit, which reduces the time of the symbol to a quarter of its initial length, consequently enhancing its overall capacity. The complex form of data symbol on the K^{th} subcarrier in each unit is represented by X_k, where k ranges from 1 to N/4. In each unit, the IFFT block receives the MSTC output to generate the OFDM signal. After the IFFT block, the *N/4* modulated sub-carriers in each unit are combined to generate the OFDM signal. Mathematically, the OFDM signal is written as (Mohammed, A., et al., 2023):

$$x_k = \frac{2}{N}\sum_{m=0}^{\frac{N}{4}-1} X_m e^{j2\pi km/\frac{N}{4}},\ 0 \le k \le \frac{N}{4} - 1. \qquad (1)$$

Where the variable *"k"* denotes the index of the time, the variable *"N"* indicates the sub-carriers number, x_k represents the k^{th} symbol for orthogonal frequency division multiplexing (OFDM), and X_m represents the m^{th} transmitted information symbol. The resulting symbols in the time domain are subjected to a parallel-to-serial (P/S) conversion process. The cyclic prefix (CP) is inserted before each OFDM signal to maintain orthogonality and minimize inter-symbol interference (ISI). The OFDM symbol with an appropriate CP is expressed in the following manner:

$$x_k^{cp} = \frac{2}{N}\sum_{m=0}^{N-1} X_m e^{j2\pi km/N}, -L_{cp} \le k \le N - 1. \qquad (2)$$

Where (L_{cp}) represents the length of CP. On the receiver side, the transmitter processes are actually carried out in the opposite sequence at the receiver side in order to recover the transmitted data. It is also important to keep in mind that the IFFT and MSTC that were employed on the transmitter side are replaced on the receiver side by the Fast Fourier Transform (FFT) and modified symbol time extension (MSTE), as shown in Figure 3.

The System Model of the MSTC

The MSTC methode is used on the side of the transmitter by using spreading and combining procedures. The MSTC approach is constructed by combining two comparable units, as seen in Figure 4.

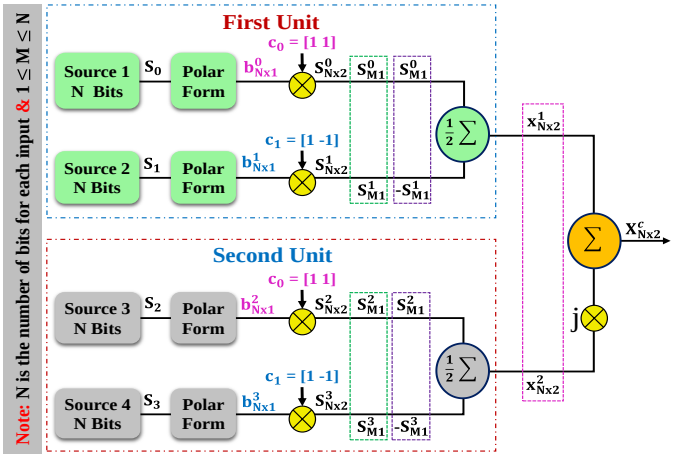

Figure 4: Schematic Presentation of the MSTC Scheme (Mohammed, A., et al., 2023)

The source data is first transformed into polar form. Then, the Walsh code (*c*), which is created utilizing the Hadamard matrix (*H*), is used to spread the polar form. The (*2x2*) Hadamard matrix is utilized in this paper, and it is presented as follows (Mohammed, A., et al., 2023):

$$\mathbf{H_{2\times 2}} = \begin{bmatrix} 1 & 1 \\ 1 & -1 \end{bmatrix} \quad (3)$$

Each column and row of the Hadamard matrix shows an individual Walsh code, where each of the spreading Walsh codes is written as follows:

$$\mathbf{c^0_{1x2}} = [1 \quad 1] \quad \& \quad \mathbf{c^1_{1x2}} = [1 \quad -1] \quad (4)$$

To generate the spread data, the polar data is multiplied by the Walsh codes as follows:

$$\begin{aligned} \mathbf{S^0_{N\times 2}} &= b^0_{N\times 1} \times c^0_{1x2}, & \mathbf{S^1_{N\times 2}} &= b^1_{N\times 1} \times c^1_{1x2}, \\ \mathbf{S^2_{N\times 2}} &= b^2_{N\times 1} \times c^0_{1x2}, & \mathbf{S^3_{N\times 2}} &= b^3_{N\times 1} \times c^1_{1x2} \end{aligned} \quad (5)$$

Where ($b^0_{N\times 1}$ & $b^1_{N\times 1}$) are the polar form and ($S^0_{N\times 2}$ & $S^1_{N\times 2}$) represent the first unit's spread data. Concerning the second unit, ($b^2_{N\times 1}$ & $b^3_{N\times 1}$) represent the polar form, while ($S^2_{N\times 2}$ & $S^3_{N\times 2}$) represent the spread data. Following the completion of the spreading process, the data obtained from the spread procedures is combined for the two units. In the first unit, the spread data ($S^0_{N\times 2}$ & $S^1_{N\times 2}$) are combined to produce the combining data $x^1_{N\times 2}$. Likewise, the spread information ($S^2_{N\times 2}$ & $S^3_{N\times 2}$) are combined in the second unit to generate the combining data $x^2_{N\times 2}$. The mathematical expression for the process of combining the first and second components is as follows:

$$\begin{aligned} x^1_{Nx2} &= \frac{1}{2}[(S^0_{M1} + S^1_{M1}) \qquad (S^0_{M1} - S^1_{M1})] \\ x^2_{Nx2} &= \frac{1}{2}[(S^2_{M1} + S^3_{M1}) \qquad (S^2_{M1} - S^3_{M1})] \\ X^c_{Nx2} &= x^1_{Nx2} + jx^2_{Nx2} \end{aligned} \quad (6)$$

As seen in Figure 4, the complex output X^c_{Nx2} is obtained by summing the imaginary part, created by multiplying the second unit's output by *"j"*, to the output of the first unit.

MSTE System Model

This sub-section provides an explanation of the mathematical analysis for the MSTE approach. First, the received signal is split into its real and imaginary components via MSTE technology. The first unit processes the real part, and the second unit treats the imaginary part, as seen in Figure 5.

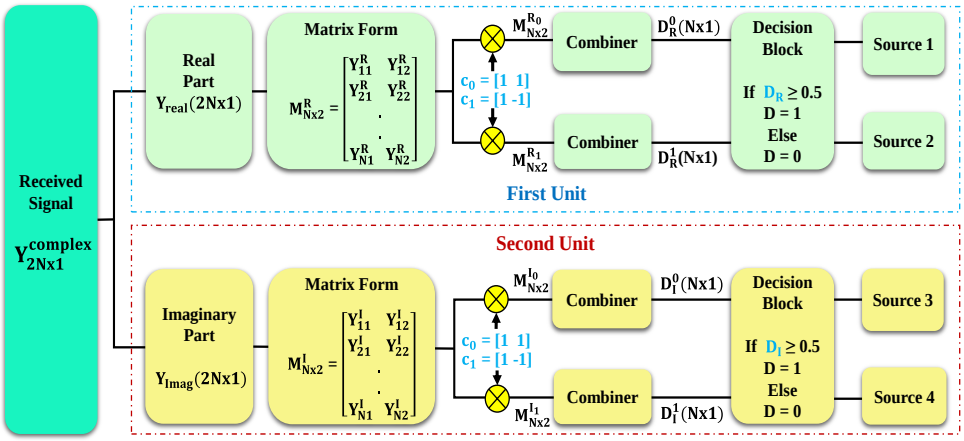

Figure 5: Schematic Presentation of the MSTE Scheme (Mohammed, A., et al., 2023)

In the first unit, the real component of the incomming signal is converted into an $N \times 2$ matrix ($\mathrm{M}^{\mathrm{R}}_{\mathrm{Nx2}}$). Thereafter, the data is spread by multiplying the Walsh codes ($\mathrm{c}^{0}_{1x2} = [1\ 0\ ;\ 0\ 1]$ & $\mathrm{c}^{1}_{1x2} = [1\ 0\ ;\ 0\ -1]$) by the matrix $\mathrm{M}^{\mathrm{R}}_{\mathrm{Nx2}}$. The combining mechanism is subsequently performed on the spread data. Mathematically, it is expressed as follows:

$$\mathbf{M}^{\mathbf{R_0}}_{\mathbf{N\times 2}} = \mathrm{M}^{\mathrm{R}}_{\mathrm{N\times 2}} \times \mathrm{c}^{0}_{1\times 2} = \begin{bmatrix} Y^{R}_{11} & Y^{R}_{12} \\ Y^{R}_{N1} & Y^{R}_{N2} \end{bmatrix}, \qquad \underbrace{\boldsymbol{D^{0}_{R}}}_{\mathbf{Nx1}} = \frac{\sum_{i=1}^{N}\left(M^{R_0}_{i1} + M^{R_0}_{i2}\right) + 1}{2},$$

$$\mathbf{M}^{\mathbf{R_1}}_{\mathbf{N\times 2}} = \mathrm{M}^{\mathrm{R}}_{\mathrm{N\times 2}} \times \mathrm{c}^{1}_{1\times 2} = \begin{bmatrix} Y^{R}_{11} & -Y^{R}_{12} \\ Y^{R}_{N1} & -Y^{R}_{N2} \end{bmatrix} \qquad \underbrace{\boldsymbol{D^{1}_{R}}}_{\mathbf{Nx1}} = \frac{\sum_{i=1}^{N}\left(M^{R_1}_{i1} + M^{R_1}_{i2}\right) + 1}{2} \tag{7}$$

Finally, the decision block receives the combined data ($\mathrm{D}^{0}_{\mathrm{R}}$ and $\mathrm{D}^{1}_{\mathrm{R}}$) and recovers the transmitted data. All steps taken in the first unit (the real part) will be repeated in the second unit (the imaginary part) in a similar manner.

3 Analysis of Simulation Results

This section presents the outcomes of the simulation performed for the proposed design, covering several performance measures, including the OFDM symbol time, BER, PAPR, and power spectral density (PSD). The modulation technique used for encoding the input information is binary phase-shift keying (BPSK). The bandwidth (BW) in this paper is 180kHz, the frequency Spacing Δf = 15kHz, the frequency sampling f = 1.92MHz, the FFT size is equal to 128, and the cyclic prefix (CP) = one-fourth of the OFDM symbol. For the channel in this article, the Rayleigh fading channel and the Additive White Gaussian Noise (AWGN) are used. The BER is calculated utilizing Monte-Carlo simulations by employing 1,000 OFDM symbols. The multi-path channel, which consists of six separate paths and is known as the Rural-Urban channel (COST207), is utilized in this communication system. The parameters of the channel, including its power and its latency, are presented in Table 1. In this paper, the frequency of the Doppler effect is ignored (i.e. the frequency of the Doppler effect is fixed to zero).

Table 1: Channel Power-Delay Profile (Mohammed, A., et al., 2019)

Rural Urban channel (COST207)						
Tap No	**1**	**2**	**3**	**4**	**5**	**6**
Power (dB)	0	-4	-8	-12	-16	-20
Delay (μs)	0	0.1	0.2	0.3	0.4	0.5

Performance Comparison of the CSTC-OFDM and MSTC-OFDM Systems

Figure 6 illustrates a performance analysis of the OFDM system using the BPSK modulation (BPSK-OFDM), the CSTC-OFDM system (Mohammed, A., El-Bakry, M., et al., 2023), and the MSTC-OFDM system (Mohammed, A., et al., 2023) in terms of a number of metrics, including the time-domain characteristics of the transmitted signal, PSD, PAPR, and BER. As shown in Figure 6 (a), the MSTC-OFDM technology minimizes the symbol time duration of the OFDM system to a quarter in comparison to the typical OFDM system (BPSK-OFDM) and to a half compared to the CSTC-OFDM system, respectively. The analysis of Figure 6 (b) reveals that reducing the symbol time leads to significant reductions in bandwidth usage for both the CSTC-OFDM and MSTC-OFDM systems. Specifically, the CSTC-OFDM system achieves bandwidth savings of up to 50%, while the MSTC-OFDM system achieves even greater savings of 75% relative to the BPSK-OFDM system. Furthermore, the utilization of the MSTC-OFDM method not only contributes to bandwidth conservation but also enhances system performance through the mitigation of the PAPR issue. Figure 6 (c) shows that the PAPR gains for the MSTC-OFDM and CSTC-OFDM systems compared to the BPSK-OFDM system are 2.11 dB and 1.11 dB, respectively. The MSTC-OFDM system has the benefit of being able to deliver the same amount of data as the CST-OFDM and BPSK-OFDM systems with a lower bandwidth and greater improvement in PAPR. However, as shown in Figure 6 (d), the BER in the MSTC-OFDM system is equal to that of the CST-OFDM and BPSK-OFDM systems.

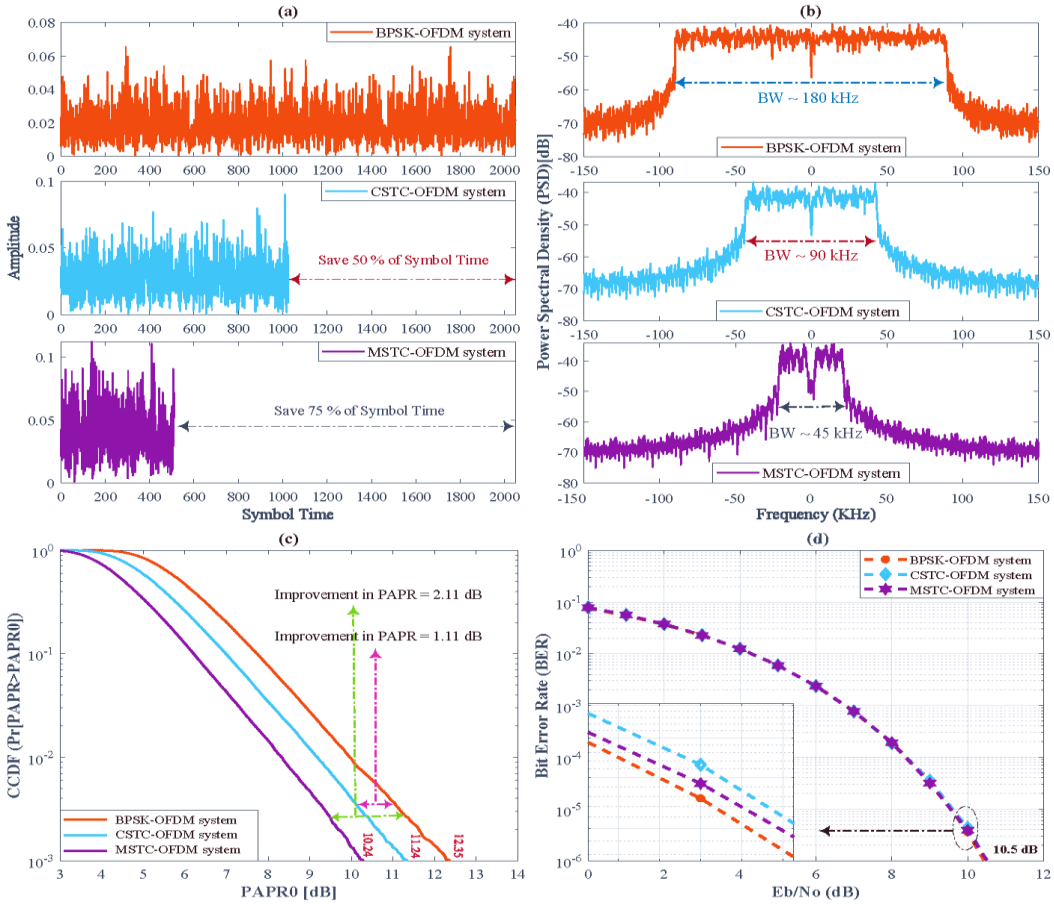

Figure 6: Comparative Analysis of the BPSK-OFDM, CSTC-OFDM, and MSTC-OFDM Systems Based on: (a) Transmitted Signal Time Domain; (b) PSD; (c) PAPR; and (d) BER

The Suggested Design (4-MSTC-OFDM) Simulation Results

This subsection explains the simulation outcomes of the suggested design (4-MSTC-OFDM), which transmits four times as much information as the conventional OFDM system. This article displays a simple implementation of the suggested design, in which a parking garage is built utilizing the suggested design and the standard OFDM approach. On the transmitter side, the camera works as the data input source, while on the receiver side, the screen is responsible for retrieving and displaying the data transmitted. Figure 7 depicts the use of a typical OFDM system to send images from a parking garage to a control unit on the receiver side, with a single camera serving as a data input source.

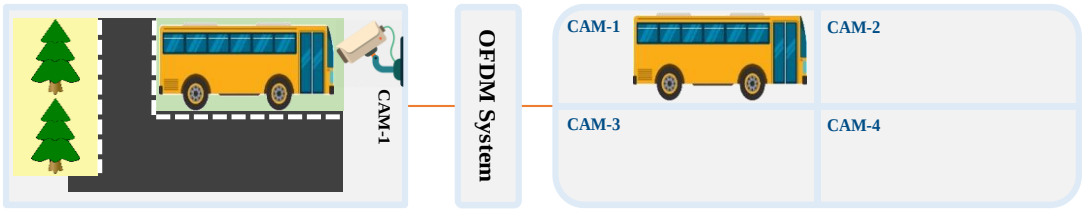

Figure 7: Sending Images from a Parking Garage using the Conventional OFDM System

Figure 8 illustrates the transmission of images from the parking garage to the control unit on the receiver side, utilizing the proposed design. The 4-MSTS-OFDM, as seen in Figure 8, employs four cameras instead of a single camera to handle and transmit data that is four times larger in amount while utilizing the same bandwidth as a conventional OFDM system.

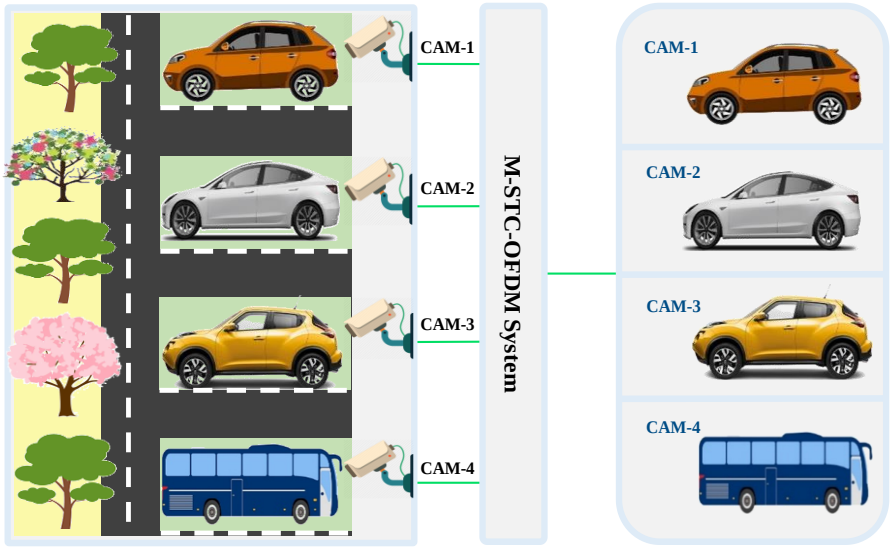

Figure 8: Transmitting 4 Pictures from a Parking Garage using the Proposed Design (4-MSTC-OFDM).

The parking garage simulation was performed using the Matlab 2021a software. In Figure 9, we simulate the transmission of pictures from the transmitter to the receiver over the AWGN channel using both the standard OFDM system and the 4-MSTC-OFDM design. Figure 9 (a) depicts the transmission of one picture via the conventional OFDM system, while Figure 9 (b) illustrates the transmission of four images using the 4-MSTC-OFDM design. Figure 9 (c) illustrates the BER performance comparison of the standard OFDM system and the 4-MSTC-OFDM design. According to Figure 9, the suggested design performs more effectively than the conventional OFDM system by transmitting four times the data using the same bandwidth while maintaining the same BER.

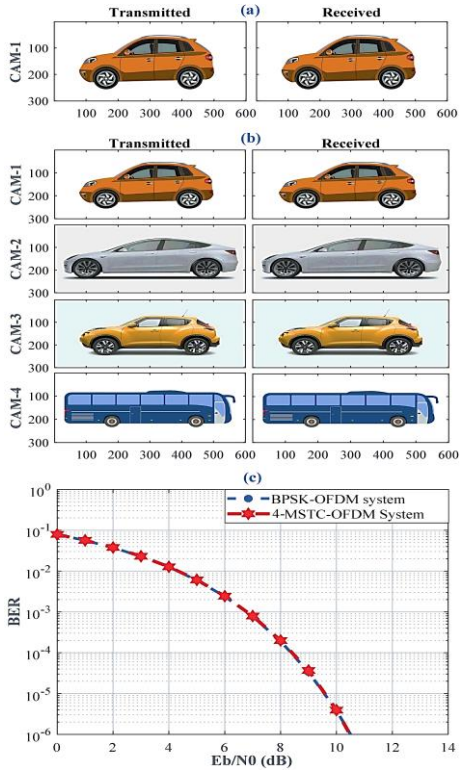

Figure 9: Comparing the Performance of the 4-MSTC-OFDM with BPSK-OFDM Based on the Amount of Transmitted Data and the BER: (a) Transmitting Pictures using BPSK-OFDM, (b) Transmitting Pictures Using 4-MSTC-OFDM, and (c) BER

Figure 10 and Figure 11 display the BER for a conventional OFDM system utilizing BPSK modulation, the CSTC-OFDM system, the proposed design (4-MSTC-OFDM), and the OFDM system using 16 QAM over AWGN and Rayleigh fading channels, respectively. According to both Figure 10 and Figure 11, the suggested design, 4-MSTC-OFDM, has the same BER as conventional OFDM and CSTC-OFDM systems. Moreover, the suggested design (4-MSTC-OFDM) decreases the SNR for transmitting the same amount of data by using the AWGN channel and Rayleigh channel (COST207), respectively, by 3.9 dB (at BER = 10-6) and 4.4 dB (at BER = 10-4) when compared to the 16-QAM-OFDM system.

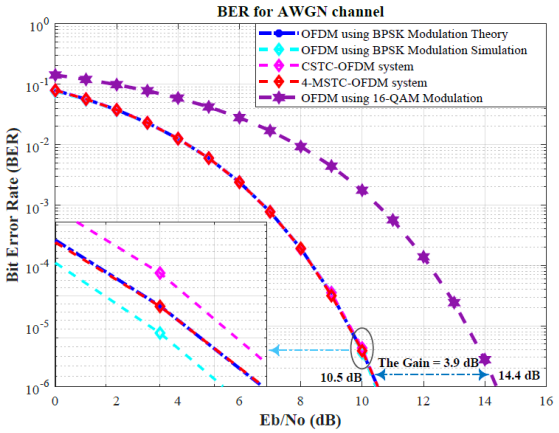

Figure 10: BER-based Performance Comparison Over AWGN Channel

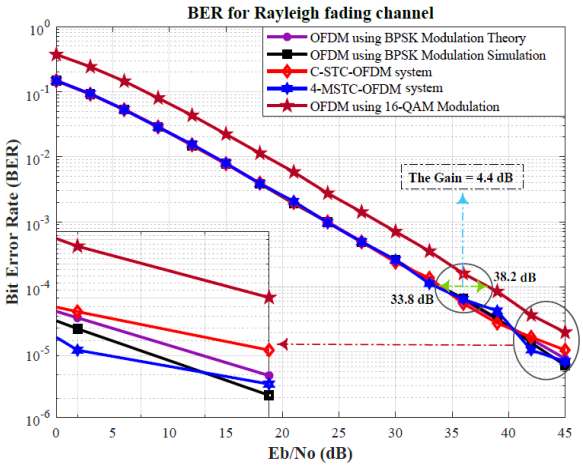

Figure 11: BER-based Performance Comparison Over Rayleigh Fading Channel (COST207)

Computational Complexity

This subsection describes the complexities of HT-Fast-OFDM and our suggested design, 4-MSTC-OFDM. The computational complexity of the FFT for additions is equal to N log2 N, while the computational complexity for multiplication is equal to $\frac{N}{2}$ log2 (Mohammed, A., et al., 2021). A number of presumptions are used to compute complexity: 1) Subtraction and addition are equally complicated; 2) division and multiplication are also equally complicated. The OFDM system demands an overall of $\frac{N}{2}\log_2(N)$ multiplications and $N\log_2(N)$ additions. In (Liu, X., & Darwazeh, I., 2019, April), the HT-Fast-OFDM system has been split into two separate components, each having N FFT points. The Hilbert transform pair (g(t) and $g^{\wedge}(t)$), has been multiplied by the two components. The g(t) is multiplied by the first component, and the $g^{\wedge}(t)$ is multiplied by the second component. The two separate portions are subsequently connected together. Consequently, the computational complexity of this system will be characterized by $N\log_2(N) + 2$ multiplications and $2N\log_2(N) + 1$ addition. Our proposed design (4-MSTC-OFDM) has the following complexity: The MSTC involves 6N addition operations and 4N multiplication, in addition to the overall complexity of OFDM. Consequently, the proposed design (4-MSTC-OFDM) requires $\frac{N}{2}\log_2(N) + 4N$ operations for multiplication and $N\log_2(N) + 6N$ for addition. Table 2 presents a comparison of the complexity between the HT-Fast-OFDM system and the 4-MSTC-OFDM design. The comparative analysis reveals that the complexity of the proposed design is clearly lower in comparison to the HT-Fast-OFDM system.

Table 2: Analysis of the Complexity

	N		**N = 128**		**N = 1024**		**N = 4096**	
	No. Multi	No. Add	No. Multi	No. Add	No. Multi	No. Add	No. Multi	No. Add
HT-Fast-OFDM	$N\log_2(N) + 2$	$2N\log_2(N) + 1$	1793	898	20481	10242	98305	49154
4-MSTC-OFDM	$\frac{N}{2}\log_2(N) + 4N$	$N\log_2(N) + 6N$	1536	960	15360	9216	69632	40960

4 Conclusion

This paper presents the 4-MSTC-OFDM design, which has the capability to transmit information at a rate that is four times greater than that of the BPSK-OFDM system. The 4-MSTC-OFDM design is

based on the MSTC scheme, which decreases the bandwidth (BW) to one-fourth of its previous value (25%) by compressing the time symbol to one-fourth (i.e. it maintains 75% of the bandwidth). The 4-MSTC-OFDM design exploits the unused bandwidth to send more data. The results of the simulation indicate that the 4-MSTC-OFDM design has the capability to deliver a quadruple amount of data compared with the BPSK-OFDM system while simultaneously preserving a similar bit error rate (BER). Furthermore, compared to the 16-QAM-OFDM system, the proposed design (4-MSTC-OFDM) decreases the SNR by 3.9 dB (at BER = 10^{-6}) and 4.4 dB (at BER = 10^{-4}) by employing the AWGN channel and Rayleigh channel (COST207), respectively. Even though the HT-Fast-OFDM system and our suggested design (4-MSTC-OFDM) are both capable of transmitting the same quantities of information, it is evident that the complexity of our proposed design is notably lesser compared to the HT-Fast-OFDM system.

References

[1] Caviglione, L., Wendzel, S., Mileva, A., & Vrhovec, S. (2021). Guest Editorial: Multidisciplinary Solutions to Modern Cybersecurity Challenges. *Journal of Wireless Mobile Networks, Ubiquitous Computing, and Dependable Applications (JoWUA), 12*(4), 1-3.

[2] Chen, Y., Sambo, Y.A., Onireti, O., & Imran, M.A. (2022). A survey on LPWAN-5G integration: Main challenges and potential solutions. *IEEE Access*, *10*, 32132-32149.

[3] Dangana, M., Ansari, S., Abbasi, Q.H., Hussain, S., & Imran, M.A. (2021). Suitability of NB-IoT for indoor industrial environment: A survey and insights. *Sensors*, *21*(16), 1-28.

[4] Du, R., Santi, P., Xiao, M., Vasilakos, A.V., & Fischione, C. (2018). The sensable city: A survey on the deployment and management for smart city monitoring. *IEEE Communications Surveys & Tutorials*, *21*(2), 1533-1560.

[5] Elbakry, M.S., Mohammed, A., & Ismail, T. (2022). Throughput improvement and PAPR reduction for OFDM-based VLC systems using an integrated STC-IMADJS technique. *Optical and Quantum Electronics*, *54*(7), 1-17.

[6] Ertürk, M.A., Aydın, M.A., Büyükakkaşlar, M.T., & Evirgen, H. (2019). A survey on LoRaWAN architecture, protocol and technologies. *Future internet*, *11*(10), 1-34.

[7] Javidroozi, V., Shah, H., & Feldman, G. (2019). Urban computing and smart cities: Towards changing city processes by applying enterprise systems integration practices. *IEEE Access*, *7*, 108023-108034.

[8] Li, Y., Chi, K., Chen, H., Wang, Z., & Zhu, Y. (2017). Narrowband Internet of Things systems with opportunistic D2D communication. *IEEE Internet of Things Journal*, *5*(3), 1474-1484.

[9] Liu, S., Xiao, L., Han, Z., & Tang, Y. (2019). Eliminating NB-IoT interference to LTE system: A sparse machine learning-based approach. *IEEE Internet of Things Journal*, *6*(4), 6919-6932.

[10] Liu, X., & Darwazeh, I. (2019). Quadrupling the data rate for narrowband internet of things without modulation upgrade. *In IEEE 89th Vehicular Technology Conference (VTC2019-Spring)*, 1-5.

[11] Luján, E., Mellino, J.A.Z., Otero, A.D., Vega, L.R., Galarza, C.G., & Mocskos, E.E. (2019). Extreme coverage in 5g narrowband iot: a lut-based strategy to optimize shared channels. *IEEE Internet of Things Journal*, *7*(3), 2129-2136.

[12] Malik, H., Alam, M.M., Pervaiz, H., Le Moullec, Y., Al-Dulaimi, A., Parand, S., & Reggiani, L. (2019). Radio resource management in NB-IoT systems: Empowered by interference prediction and flexible duplexing. *IEEE Network*, *34*(1), 144-151.

[13] Marini, R., Mikhaylov, K., Pasolini, G., & Buratti, C. (2022). Low-power wide-area networks: Comparison of LoRaWAN and NB-IoT performance. *IEEE Internet of Things Journal*, *9*(21), 21051-21063.

[14] Martinez, B., Adelantado, F., Bartoli, A., & Vilajosana, X. (2019). Exploring the performance boundaries of NB-IoT. *IEEE Internet of Things Journal*, *6*(3), 5702-5712.
[15] Mekki, K., Bajic, E., Chaxel, F., & Meyer, F. (2019). A comparative study of LPWAN technologies for large-scale IoT deployment. *ICT express*, *5*(1), 1-7.
[16] Migabo, E.M., Djouani, K.D., & Kurien, A.M. (2020). The narrowband Internet of Things (NB-IoT) resources management performance state of art, challenges, and opportunities. *IEEE Access*, *8*, 97658-97675.
[17] Mohammed, A., El-Bakry, M., Mostafa, H., & Ammar, A.E.H.A. (2022). Doubling the number of connected devices in narrow-band internet of things while maintaining system performance: An stc-based approach, 1-9.
[18] Mohammed, A., Ismail, T., Nassar, A., & Mostafa, H. (2021). A novel companding technique to reduce high peak to average power ratio in OFDM systems. *IEEE Access*, *9*, 35217-35228.
[19] Mohammed, A., Mostafa, H., & Ammar, A.A. (2023). An effective technique for increasing capacity and improving bandwidth in 5G narrow-band internet of things. *International Journal of Electrical and Computer Engineering (IJECE)*, *13*(5), 5232-5242.
[20] Mohammed, A., Shehata, M., Mostafa, H., & Nassar, A. (2018). Peak-to-average power ratio suppression using companding schemes in OFDM systems. *In IEEE 61st International Midwest Symposium on Circuits and Systems (MWSCAS)*, 933-936.
[21] Mohammed, A., Shehata, M., Nassar, A., & Mostafa, H. (2019). Performance comparison of companding-based papr suppression techniques in ofdm systems. *In IEEE 8th International Conference on Modern Circuits and Systems Technologies (MOCAST)*, 1-4.
[22] Nair, V., Litjens, R., & Zhang, H. (2019). Optimisation of NB-IoT deployment for smart energy distribution networks. *Eurasip journal on wireless communications and networking*, *2019*, 1-15.
[23] Niu, Y., Gao, C., Li, Y., Su, L., Jin, D., & Vasilakos, A.V. (2015). Exploiting device-to-device communications in joint scheduling of access and backhaul for mm Wave small cells. *IEEE Journal on Selected Areas in Communications*, *33*(10), 2052-2069.
[24] Qolomany, B., Al-Fuqaha, A., Gupta, A., Benhaddou, D., Alwajidi, S., Qadir, J., & Fong, A.C. (2019). Leveraging machine learning and big data for smart buildings: A comprehensive survey. *IEEE Access*, *7*, 90316-90356.
[25] Wan, L., Zhang, Z., & Wang, J. (2019). Demonstrability of Narrowband Internet of Things technology in advanced metering infrastructure. *EURASIP Journal on Wireless Communications and Networking*, *2019*, 1-12.
[26] Xu, T., & Darwazeh, I. (2018). Non-orthogonal narrowband Internet of Things: A design for saving bandwidth and doubling the number of connected devices. *IEEE Internet of Things Journal*, *5*(3), 2120-2129.
[27] Xu, T., & Darwazeh, I. (2018, September). Uplink narrowband IoT data rate improvement: Dense modulation formats or non-orthogonal signal waveforms? *In IEEE 29th Annual International Symposium on Personal, Indoor and Mobile Radio Communications (PIMRC)*, 142-146.
[28] Zuniga, J.C., & Ponsard, B. (2016). Sigfox system description. *LPWAN@ IETF97, Nov. 14th*, *25*, 14.

Authors Biography

Abdulwahid Mohammed received the B.S. degree in Electronics and Communication Engineering from Saad Dahlab University, Algeria, in 2010, and the M.S. degree in Electronics and Communication Engineering from Cairo University, Egypt, in 2019. During his Master's study, Abdulwahid worked as a research assistant in the Opto-Nanoelectronics Laboratory (One LAB), Department of Electronics and Communications, Faculty of Engineering, Cairo University, Egypt. He is currently pursuing the Ph.D. degree in Electronics and Communication Engineering from Al-Azhar University, Egypt. He worked as a research assistant at the Smart Engineering Systems Research Center (SESC), Faculty of Engineering, and Nile University, Egypt. His research interests include NB-IoT, wireless communication systems, 5G/6G communication networks, and artificial intelligence. He can be contacted at email: abdulwahid1520121@eng1.cu.edu.eg.

Hassan Mostafa received the B.Sc. and M.Sc. degrees (Hons.) in electronics engineering from Cairo University, Cairo, Egypt, in 2001 and 2005, respectively, and the Ph.D. degree in electrical and computer engineering from the Department of Electrical and Computer Engineering, University of Waterloo, Waterloo, ON, Canada, in 2011. He is currently an Associate Professor with the Nanotechnology and Nano-electronics Program, Zewail City of Science and Technology, Giza, Egypt, on leave from the Department of Electronics and Electrical Communications, Cairo University. He was an NSERC Postdoctoral Fellow with the Department of Electrical and Computer Engineering, University of Toronto, Toronto, ON, Canada. He was a Postdoctoral Researcher in collaboration with Fujitsu Research Laboratories in Japan and USA with a focus on the design of the next-generation FPGA. He has authored/coauthored more than 300 articles in international journals and conferences and five published books. His research interests include neuromorphic computing, the IoT hardware security, software-defined radio, reconfigurable low-power systems, analog-to-digital converters, low-power circuits, subthreshold logic, variation-tolerant design, soft error-tolerant design, statistical design methodologies, next-generation FPGA, spintronics, memristors, energy harvesting, MEMS/NEMS, power management, and optoelectronics. He has been a member of the IEEE Technical Committee of VLSI Systems and Applications since 2017. He was a recipient of the University of Waterloo Sand Ford Fleming TA Excellence Award in 2008, the Ontario Graduate Scholarship in 2009, the Waterloo Institute of Nano- Technology Nano fellowship Research Excellence Award in 2010, the Natural Sciences and Engineering Research Council of Canada Prestigious Postdoctoral Fellowship in 2011, and the University of Toronto Research Associate Scholarship in 2012. He can be contacted at email: hmostafa@uwaterloo.ca.

Abdelhady Abdelazim Ammar received the B.Sc. degree in Electronics and Communication Engineering from Alex University, Egypt, in 1963, the DEA and Ph.D. degrees from Paris University, France, in June 1965 and Dec 1968, respectively. He joined nuclear Engineering Department, in Madison Wisconsin, USA for two years from 1969 to 1971. He is a professor in Electronics and Communications Engineering department, Faculty of Engineering, Al-Azhar University, Cairo, Egypt since 1988. His research activities are within digital communications, mobile communications and digital signal processing. He can be contacted at email: hady42amar@gmail.com.